Comments on Inorganic Chemistry
Publication details, including instructions for authors and subscription information:
http://www.informaworld.com/smpp/title~content=t713455155

Quantification of Intramolecular Ligand Equilibria in Metal-Ion Complexes

R. Bruce Martin[a]; Helmut Sigel[b]
[a] Chemistry Department, University of Virginia, Charlottesville, Virginia [b] Institute of Inorganic Chemistry, University of Basel, Basel, Switzerland

To cite this Article Martin, R. Bruce and Sigel, Helmut(1988) 'Quantification of Intramolecular Ligand Equilibria in Metal-Ion Complexes', Comments on Inorganic Chemistry, 6: 5, 285 — 314
To link to this Article: DOI: 10.1080/02603598808072294
URL: http://dx.doi.org/10.1080/02603598808072294

Quantification of Intramolecular Ligand Equilibria in Metal-Ion Complexes

That in a metal-ion chelate one binding site may be more weakly bound than another is often expected, though it is not equally well realized that such differences in metal-ion affinities may give rise to intramolecular equilibria between open and closed, i.e., chelated, forms. Quantification procedures for such equilibria are outlined and applied to describe the situation in complexes of N-substituted iminodiacetate and α-substituted acetate ligands. Corresponding procedures are applicable to the characterization of intramolecular ligand–ligand interactions in mixed ligand complexes. Isomerization equilibria are of general importance; e.g., in metal-ion catalyzed or facilitated technical or biological processes.

1. INTRODUCTION

The difference in intensity with which certain donor atoms bind to a metal ion has long fascinated coordination chemists. Schwarzenbach with his co-workers[1] considered the intramolecular equilibrium (1)

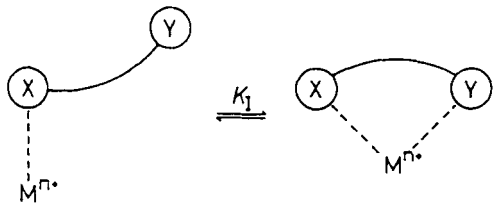

(1)

in solution for metal ion (M^{n+}) complexes of ligands (L) having a strong binding site X and a more weakly coordinating one Y;

Comments Inorg. Chem.
1988, Vol. 6, Nos. 5 & 6, pp. 285–314
Photocopying permitted by license only

the resulting isomeric complexes are termed open isomer, ML_o, and chelated or closed isomer, ML_{cl}. The same authors[1] have also given expression (2),

$$K_I = \frac{K^M_{ML}}{K^M_{ML_o}} - 1 \qquad (2)$$

where K^M_{ML} represents the overall formation constant (see Section 2) and $K^M_{ML_o}$ the stability of the open isomer.

Expression (2) has been derived independently by a number of workers (e.g., Refs. 2 and 3), but it was Mariam and Martin[4] who first exploited this expression and calculated the percentage of the macrochelated isomers of several Ni^{2+}/nucleotide complexes. This application has since been extended to complexes of other nucleotides[5–7] and nucleotide derivatives,[8] as well as to complexes of thioether ligands[9] and related substances of biological interest like derivatives of *d*-biotin[10] or α-lipoic acid.[11] Related evaluations are also possible for intramolecular ligand–ligand interactions in mixed ligand complexes.[12–14]

This Comment aims to emphasize the general importance of equilibrium (1), to develop a sense of where it matters, e.g., in catalytic or biological reactions, and to provide the necessary background information. Such information serves to indicate the calculation procedures and to evaluate the intrinsic properties of this equilibrium, including the relations between complex stability, the degree of formation of the closed species, and the effects on the free energy (ΔG^0).

2. RELATIONS FOR INTRAMOLECULAR EQUILIBRIA AND DEFINITION OF THE STABILITY ENHANCEMENT (*E*)

Any metal ion may combine with a suitable and deprotonated ligand to produce the isomeric complexes shown in equilibrium (1); i.e., to give open and closed complexes according to equilibrium (3) (charges omitted for clarity):

$$M + L \rightleftharpoons ML_o \rightleftharpoons ML_{cl} \qquad (3)$$

We define the equilibrium constant for the formation of the open complex by Eq. (4),

$$K^{M}_{ML_o} = [ML_o]/([M][L]) \tag{4}$$

and the unitless equilibrium constant for isomerization of the open to the closed complex by Eq. (5):

$$K_I = [ML_{cl}]/[ML_o] \tag{5}$$

The observed (overall) equilibrium constant, K^{M}_{ML}, over both open and closed species is then given by Eq. (6):

$$K^{M}_{ML} = \frac{([ML_o] + [ML_{cl}])}{[M][L]} = K^{M}_{ML_o} + K_I \cdot K^{M}_{ML_o} = K^{M}_{ML_o}(1 + K_I) \tag{6}$$

The presence of any closed form will enhance complex stability. Analogous to the concept of enhancement in physical chemistry as in the nuclear Overhauser effect enhancement,[15] the stability enhancement E may be defined[16] by Eq. (7),

$$E = K_I = \frac{K^{M}_{ML} - K^{M}_{ML_o}}{K^{M}_{ML_o}} = \frac{K^{M}_{ML}}{K^{M}_{ML_o}} - 1 \tag{7}$$

which encompasses Eq. (2).[9,11] Consequently, the so-called stability enhancement factor $(1 + E)$ is given by the relation (8):

$$1 + E = \frac{K^{M}_{ML}}{K^{M}_{ML_o}} = 10^{\log(K^{M}_{ML}/K^{M}_{ML_o})} \tag{8}$$

This stability enhancement factor is also often expressed[5–11] as $10^{\log\Delta}$ because it equals the difference between the logarithms of two stability constants:

$$\log \Delta = \log K^{M}_{ML} - \log K^{M}_{ML_o} = \log(1 + E) \tag{9}$$

Obviously the reliability of any calculations for E or K_1 (Eq. (7)) depends on the accuracy of this difference, and this accuracy largely depends on the experimental error in the constants, which becomes more important the more similar the two constants are in Eq. (9).

The stability enhancement factor may be obtained by comparing the observed stability constant of the complex with that expected for the corresponding complex without a closed form. Often the comparison is made by plotting for a series of complexes the values of log K^{M}_{ML} versus the pK^{H}_{HL} values (Eq. (10)) of

$$HL \rightleftharpoons H^+ + L^- \qquad K^{H}_{HL} = ([H^+][L^-])/[HL] \qquad (10)$$

the corresponding ligands; for a series of complexes with structurally related ligands a straight line often results.[17] Such an example is shown in Fig. 1[18]: the data for the Cu^{2+} 1:1 complexes of simple carboxylates fit on a straight line with a slope of 0.424 $\pm$ 0.032 (2σ), while the stability of the Cu^{2+} 1:1 complexes with tetrahydrofuran-2-carboxylate ($Thfc^-$) and tetrahydrothiophene-2-carboxylate ($Thtc^-$) is considerably larger than expected from the basicity of the carboxylate group (pK^{H}_{HL}) for a pure carboxylate coordination (ML_o). This result shows that equilibrium (1) is operating, and that the oxygen of the tetrahydrofuran group and the sulfur of the tetrahydrothiophene ring to some extent also coordinate to Cu^{2+}. The values for the logarithms of the corresponding enhancement factors (1 + E) for the two complexes are represented by the two broken vertical lines in Fig. 1. Clearly the enhancement factor is that by which the baseline stability constant, $K^{M}_{ML_o}$ (which is defined by pK^{H}_{HL}; Fig. 1) should be multiplied to give the observed stability constant, K^{M}_{ML} (see Eq. (8)). For $Cu(Thfc)^+$ and $Cu(Thtc)^+$ these factors correspond to $10^{0.80}$ and $10^{1.12}$, respectively.

3. RELATIONSHIP BETWEEN STABILITY ENHANCEMENT, FRACTION OF THE CLOSED COMPLEX, AND THE FREE ENERGY

Equilibria (1) and (3) show that with a potentially chelating ligand the fraction of closed complexes (ML_{cl}) may range from zero, where all complexes are open (ML_o), to nearly unity, where vir-

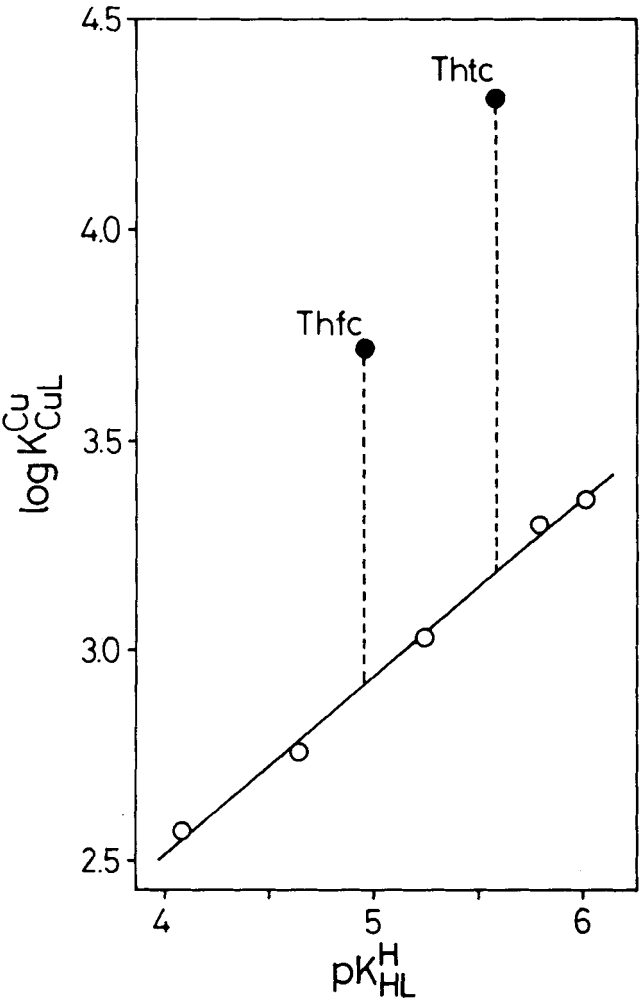

FIGURE 1 Relationship between log K^{Cu}_{CuL} and pK^{H}_{HL} for the Cu^{2+} 1:1 complexes of the monodentate carboxylates (○) (from left to right) chloroacetate, p-nitrobenzoate, m-chlorobenzoate, benzoate and acetate; least-squares line: $y = (0.424 \pm 0.016)x + (0.819 \pm 0.084)$ ($\pm 1\sigma$). For comparison are also inserted the corresponding data for the complexes of the potentially bidentate ligands tetrahydrofuran-2-carboxylate ($Thfc^-$) and tetrahydrothiophene-2-carboxylate ($Thtc^-$); the vertical broken lines represent the values of log(1 + E) for $Cu(Thfc)^+$ and $Cu(Thtc)^+$; see text in Section 2. The plotted equilibrium constant values are from Table 2 of Ref. 18; they refer to 50% (v/v) aqueous dioxane solutions at 25°C and I = 0.1 M, $NaClO_4$.

tually all complexes are closed. The fraction of closed complexes, f, is given by Eq. (11):

$$f = \frac{[ML_{cl}]}{[ML_o] + [ML_{cl}]} = \frac{E}{1 + E} = \frac{K_I}{1 + K_I} \qquad (11)$$

Evidently $f \cdot 100$ results in the percentage for the closed isomer of the concentration-independent equilibrium (1). The relation between the stability enhancement factor $1 + E$ ($= 10^{\log\Delta}$; see Eq. (9)) and the fraction of the closed isomer f is defined by expression (12):

$$1 + E = \frac{1}{1 - f} \qquad (12)$$

Figure 2 shows a plot of $\log(1 + E)$ on the left-hand ordinate versus f. In developing a sense of the relation between $\log(1 + E)$ and the percentage of the closed form, it should be remembered that $f \cdot 100 = \%\ ML_{cl}$. The contribution of closed complexes to the free energy change for complex formation is given by $-\Delta G^0 = RT \ln(1 + E)$. Values for the corresponding free energy change in kJ/mol at 20°C are indicated on the right-hand ordinate in Fig. 2.

Figure 2 demonstrates that when half the complexes are closed, $\log(1 + E) = 0.30$ and $\Delta G^0 = -1.7$ kJ/mol at 20°C; when 90% are closed, i.e., $f = 0.90$, $\log(1 + E) = 1.0$ and $\Delta G^0 = -5.6$ kJ/mol, and when 99% are closed ($f = 0.99$) $\log(1 + E) = 2.0$ and $\Delta G^0 = -11.2$ kJ/mol; this last situation corresponds to the position of the arrowhead in Fig. 2. Thus to close the last small fraction of open complexes, ML_o, demands ever-increasing energy and requires tight binding. On the other hand, for the closure of small amounts of complexes the required energy is weak: e.g., $\Delta G^0 = -0.56$ kJ/mol corresponds to $\log(1 + E) = 0.1$ and a formation degree of already 20% for the closed species. Hence, the presence of a relatively weak binding site in a ligating molecule may well have an effect on the structure of the complex in solution; i.e., isomeric equilibria may be initiated.

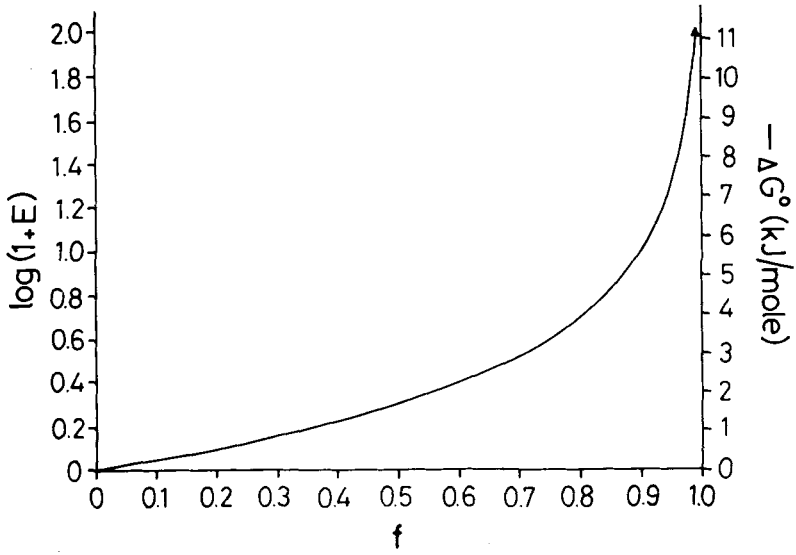

FIGURE 2 Plot of logarithm of the enhancement factor, $\log(1 + E)$, on the left-hand ordinate versus fraction of closed complexes, f. It should be remembered that $f \cdot 100$ gives the percentage of the closed complexes (cf. Section 3). The right-hand ordinate indicates the values in kJ/mol at 20°C for the contribution of closed complexes, ML_{cl}, to the free energy change for complex formation. The arrowhead resides at the point for 0.99 mol fraction of closed complexes, which corresponds to $\log(1 + E) = 2.0$ and $\Delta G^\circ = -11.2$ kJ/mol.

4. SOME COMMENTS ON THE CORRELATION *BETWEEN COMPLEX STABILITY AND LIGAND* BASICITY

As indicated in Section 2, one of the problems in applying Eq. (7) and the other relations derived from it, is the fact that values for $K^{M}_{ML_o}$ are usually not directly accessible. A common solution to this problem is to apply $\log K^{M}_{ML}$ versus pK^{H}_{HL} plots (Fig. 1). Hence, before examples regarding equilibrium (1) are considered in detail and the reasonings of Sections 2 and 3 are applied, it seems appropriate to present more background information about such baseline plots.

The linear relationship between $\log K^{M}_{ML}$ and pK^{H}_{HL} for a series

of structurally related ligands as expressed[19] by

$$\log K^{M}_{ML} = a \cdot pK^{H}_{HL} + b \tag{13}$$

has a long empiric history.[1,17,19,20] A general relationship formulated by Irving and Rossotti is given in Eq. (14) (ignoring the activity coefficients)[21]:

$$\log K^{M}_{ML} = pK^{H}_{HL} - (2.303/RT)[(G^{0}_{ML} - G^{0}_{HL}) + (G^{0}_{H} - G^{0}_{M})] \tag{14}$$

This expression was reformulated by Williams *et al.*[22] into Eq. (15),

$$\begin{aligned} \log K^{M}_{ML} &= pK^{H}_{HL} - (2.303/RT)(G^{0}_{ML} - G^{0}_{HL}) + B \\ y &= mx + b \end{aligned} \tag{15}$$

where B is a constant because G^{0}_{H} is constant, as is G^{0}_{M} for a given metal ion. Hence, a linear relationship between $\log K^{M}_{ML}$ and pK^{H}_{HL} results if the term $(G^{0}_{ML} - G^{0}_{HL})$ is negligible, constant, or, for a slope other than unity, a linear function of pK^{H}_{HL}. Since one of these three conditions usually occurs, straight lines are often observed though negative slopes are known,[23] as are curves for cases where the term $(G^{0}_{ML} - G^{0}_{HL})$ is not a linear function of pK^{H}_{HL}.[22]

Though the above information seems to suffice regarding the use of $\log K^{M}_{ML}$ versus pK^{H}_{HL} relationships as baselines for the evaluations in Sections 5 and 6 (and hurried readers may continue there), some additional thought on linear log stability constant relationships may deepen our understanding of the situation.

A linear $\log K^{M}_{ML}$ versus pK^{H}_{HL} plot for a single metal ion with a ligand family implies certain relations with a linear $\log K^{M}_{MA}$ versus $\log K^{M}_{MB}$ plot for two different ligands A and B with a variety of metal ions. For i metal ions and j ligands the stability constant for the first linear plot is represented by Eq. (16),

$$\log K^{M_i}_{M_iL_j} = \log K^{M_i}_{M_iL_0} + B_{M_i}(pK^{H}_{HL_j} - pK^{H}_{HL_0}) \tag{16}$$

where the subscript zero applies to the reference ligand, L_0, which may form only ML_o type complexes (cf. Eq. (3)). For a series of substituted ligands, which also may form ML_{cl}-type complexes, Eq. (16) becomes a Hammett-type expression,

$$\log K^{M_i}_{M_iL_j} = \log K^{M_i}_{M_iL_o} + \rho_{M_i}\sigma_{L_j} \tag{17}$$

where σ_{L_j} is a substituent constant. B_{M_i} and ρ_{M_i} represent the slopes of the log $K^{M_i}_{M_iL_j}$ versus $pK^{H}_{HL_j}$ or σ_{L_j} plots from Eqs. (16) or (17) for a single metal ion. The subscript i on B_{M_i} and ρ_{M_i} indicates that each metal ion will generally yield a different slope.

The linear free-energy relation for two different ligands with a variety of metal ions is given by

$$\log K^{M_i}_{M_iL_j} = \log K^{M_0}_{M_0L_j} + C_{L_j}(\log K^{M_i}_{M_iL} - \log K^{M_0}_{M_0L}) \tag{18}$$

where the subscript zero designates the reference metal ion. The subscript j on C_{L_j} indicates that each ligand will yield a different slope.

Analogous to earlier treatments of linear free-energy relations for reactivities, nucleophilicities, and catalytic capabilities,[24] for the pair of Eqs. (16) and (18) we perform a double differentiation and obtain Eq. (19):

$$\frac{\delta B_{M_i}}{\delta \log K^{M_i}_{M_iL}} = \frac{\delta^2 \log K^{M_i}_{M_iL_j}}{\delta pK^{H}_{HL_j}\, \delta \log K^{M_i}_{M_iL}} = \frac{\delta C_{L_j}}{\delta pK^{H}_{HL_j}} \tag{19}$$

The first equality arises from Eq. (16), the second from Eq. (18). A similar double differentiation of Eqs. (17) and (18) yields Eq. (20):

$$\frac{\delta \rho_{M_i}}{\delta \log K^{M_i}_{M_iL}} = \frac{\delta^2 \log K^{M_i}_{M_iL_j}}{\delta \sigma_{L_j}\, \delta \log K^{M_i}_{M_iL}} = \frac{\delta C_{L_j}}{\delta \sigma_{L_j}} \tag{20}$$

The left-hand sides of Eqs. (19) and (20) depend only upon the i

metal ions and the right-hand sides only on the j ligands. Thus the two sides of Eqs. (19) and (20) vary independently. According to Eq. (19), a plot of slopes B_{M_i} versus log $K^{M_i}_{M_iL}$ for a series of metal ions yields the same slope as a plot of the slopes C_{L_j} versus $pK^{H}_{HL_j}$ for a series of ligands. The same results of Eqs. (19) and (20) have also been obtained by a different approach.[25] Examples of this relationship (Eq. (19)) or the analogous one with Eq. (20) are demonstrated for both substituted pyridines and salicylaldehydes by Nieboer and McBryde.[25,26]

5. EXTENT OF SIDE-CHAIN INTERACTIONS IN COMPLEXES OF N-SUBSTITUTED IMINODIACETATES

To demonstrate the power and general applicability of the analysis described in Sections 2 and 3 for the quantification of intramolecular equilibria in metal-ion complexes (Eq. (1)), we selected the results obtained by Schwarzenbach *et al.*[1,27] for a series of complexes with N-substituted iminodiacetate ligands. The structures of these iminodiacetate derivatives and the numbering system applied here for the ligands are summarized in Fig. 3.

The equilibrium constants determined by Schwarzenbach *et al.*[1,27] and used for the calculations herein are listed in Table I. Before the position of equilibrium (1) for the complexes of those iminodiacetate ligands which carry a potential binding site in their side-chain can be considered according to Eq. (8), it is necessary to estimate stability constants for ML_o, i.e., to quantify the stability of the open isomer in which the metal ion is only coordinated to the imino nitrogen and the oxygens of the two carboxylate groups (Fig. 3). The systems with iminodiacetate or N-methyliminodiacetate cannot be directly applied in the comparisons as the proton affinity of the imino nitrogen in these ligands varies. As indicated in Section 2, baseline plots like the one given in Fig. 1 may be used to overcome this difficulty. Therefore, the procedure employed here to obtain such plots for the complexes of the iminodiacetate derivatives is described next. The reader not interested in these details may continue with Section 5.2.

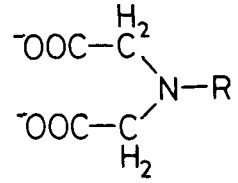

No.	Side Chain, R
I	$-CH_3$
II	$-(CH_2)_2-C(CH_3)_3$
III	$-(CH_2)_2-{}^{+}N(CH_3)_3$
IV	$-(CH_2)_2-NH-C(O)-O-C_2H_5$
V	$-CH_2-CH_2-OH$
VI	$-CH_2-CH_2-O-CH_3$
VII	$-CH_2-C(O)-NH_2$
VIII	$-CH_2-COO^-$
IX	$-CH_2-CH_2-NH_2$
X	$-CH_2-CH_2-S-CH_3$
XI	$-CH_2-CH_2-S^-$
XII	$-CH_2-CH_2-COO^-$
XIII	$-CH_2-CH_2-SO_3^-$
XIV	$-CH_2-PO_3^{2-}$
XV	$-CH_2-CH_2-PO_3^{2-}$

FIGURE 3 Structures of the N-substituted iminodiacetate ligands considered in Section 5 of this Comment. The numbers given with the substituents are those used in the text for identifying a certain derivative.

5.1 Construction of the Baseline Plots log K^{M}_{ML} versus pK^{H}_{HL}

The pK^{H}_{HL} values used in the plots correspond to deprotonation from the imino nitrogen of the monoprotonated iminodiacetate function. The $pK^{H}_{H_3L}$ and $pK^{H}_{H_2L}$ values for deprotonation of the two α-carboxylic acid groups are omitted. These latter values are not known precisely for all ligands of Fig. 3, and in any case they do not vary greatly, i.e., $pK^{H}_{H_3L}$ = 1.9 to 2.1 and $pK^{H}_{H_2L}$ = 2.1 to 2.5,[1,27] so that their influence would remain small.

Clearly, the imino nitrogen pK^{H}_{HL} required for the plots is that for the species undergoing coordination upon proton loss from the

TABLE I

Negative logarithms of the acidity constants, K^{H}_{HL} (Eq. (10)), of the N-substituted iminodiacetates of Fig. 3 and logarithms of the stability constants, K^{M}_{ML} (Eqs. (3) and (6)), of corresponding ML complexes. The equilibrium constants have been determined by Schwarzenbach *et al.* (Refs. 1 and 27) in water at 20°C and I = 0.1 M (KCl; with Cd^{2+} and Pb^{2+} KNO_3 was used)[a]

Ligand No.	pK^{H}_{HL}	log K^{M}_{ML}												
		Mg^{2+}	Ca^{2+}	Sr^{2+}	Ba^{2+}	Mn^{2+}	Fe^{2+}	Co^{2+}	Ni^{2+}	Cu^{2+}	Zn^{2+}	Cd^{2+}	Pb^{2+}	Hg^{2+}
I	9.65	3.44	3.75	2.85	2.59	5.40	6.65	7.62	8.73	11.09	7.66	6.77	8.02	5.47
II	10.24	3.60	3.68	2.70	2.41	5.55		7.78	8.70	11.49	7.92	7.12	8.16	5.91
III	5.45	1.42	1.88	1.22	1.34	2.87		5.51	~6	7.73	5.34	4.62	5.40	2.77
IV	8.57	2.68	2.99	2.14	2.00	4.60		6.71	7.94	10.50[b]	6.86	5.86	7.25	4.5
V	8.73	3.44	4.63	3.77	3.42	5.55	6.78	7.90	9.28	11.86	8.33	7.52	9.41	5.48
VI	8.96	3.31	4.53	3.84	3.56	5.53	6.81	7.96	9.39	12.34	8.43	7.53	9.49	5.94
VII	6.60	2.47	3.96	3.03	2.88	4.93		6.91	8.02	9.68	7.30	7.08	8.40	3.82
VIII	9.73	5.41	6.41	4.98	4.82	7.44	8.83	10.38	11.53	12.96	10.67	9.83	11.39	
IX	7.8[b]	4.53	4.63	3.55	3.19	7.71	9.81	11.78	13.73	15.90	11.93	10.58	12.22	9.75
X	8.91	3.02	3.34	2.71	2.62	5.10	7.12	8.51	10.00	12.63	8.28	7.89	9.12	8.01
XI	10.70[b]	4.32	4.88	3.62	3.55	9.32	11.72	14.67[c]	13.75	-[d]	15.92	16.72	17.03	16.16
XII	9.66	5.28	5.04	3.87	3.40									
XIII	8.16	3.48	4.15	3.26	3.01									
XIV	10.76	6.28	7.18	5.59	5.35									
XV	10.46	6.33	5.44	4.10	3.64									

[a]The data are collected from Table 1 of Ref. 1 (I–XI) and from Tables 1 and 3 of Ref. 27 (XII–XV). The precision of the constants was estimated by Schwarzenbach *et al.* as ±0.1 log units.

[b]See text in Section 5.1.

[c]This value does not fit the general pattern; probably oxidation occurred.

[d]A redox reaction occurs in this system (Ref. 1).

imino nitrogen. In two cases this pK^{H}_{HL} value is not measured directly because the side-chain contains a more basic group. In the case of the ethyl sulfide side-chain (XI) Schwarzenbach *et al.*[1] used the corresponding methyl thioether to resolve the microconstant equilibria (see page 1155 of Ref. 1). This widely used procedure is adopted here with the result that $pK^{H}_{HL} = 10.70$ for imino nitrogen deprotonation from the ligand with an ionized $-CH_2CH_2S^-$ side-chain.

For ligand IX with an ethylamine side-chain, Schwarzenbach *et al.*[1] set an identical pK_a for the two nitrogen deprotonations. This identity is improbable because the side-chain amino nitrogen should be much more basic than the imino nitrogen. This assertion is proved by ligand III with an ethyl betaine side-chain where $pK^{H}_{HL} = 5.45$ for the protonated imino nitrogen. A similar value applies to a protonated ethylammonium side-chain, and we assign the observed low $pK_a = 5.58$ for ligand IX to the imino nitrogen deprotonation and the observed high $pK_a = 11.05$ to the ethylammonium side-chain deprotonation. What is required, however, is the pK^{H}_{HL} for the imino nitrogen when the amino nitrogen is deprotonated. To resolve the microconstant equilibria, we add 2.2 log units to 5.58 to obtain $pK^{H}_{HL} = 7.8$, the desired value for ligand IX. The added 2.2 log units correspond to the reciprocal effects of the two ammonium group deprotonations in 1,2-diaminoethane. A similar analysis has been applied successfully to 2,3-diaminopropanoate.[28]

The baseline for the log K^{M}_{ML} versus pK^{H}_{HL} plot is taken as a linear least-squares fit for the four iminodiacetates with noncoordinating side-chains that appear as the first four ligands in Fig. 3 and in Table I. Four representative examples of such plots are shown in Figs. 4 and 5; the baselines are drawn in each case through the crossed circles (⊗). The slope of the least-squares lines through the data for the mentioned iminodiacetate derivatives with noncoordinating side-chains for all thirteen metal ions is given in the fifth row of Table II. Except for Cu^{2+} (see next paragraph) the standard deviation in the slope values varies from ± 0.03 to ± 0.06.

Table II lists the deviations from the least-squares lines for each metal ion and the ligands I to IV (Fig. 3). The points for ligand IV, which has a bulky side-chain, usually lie somewhat below the least-squares lines with only the point for Cu^{2+} giving a strong

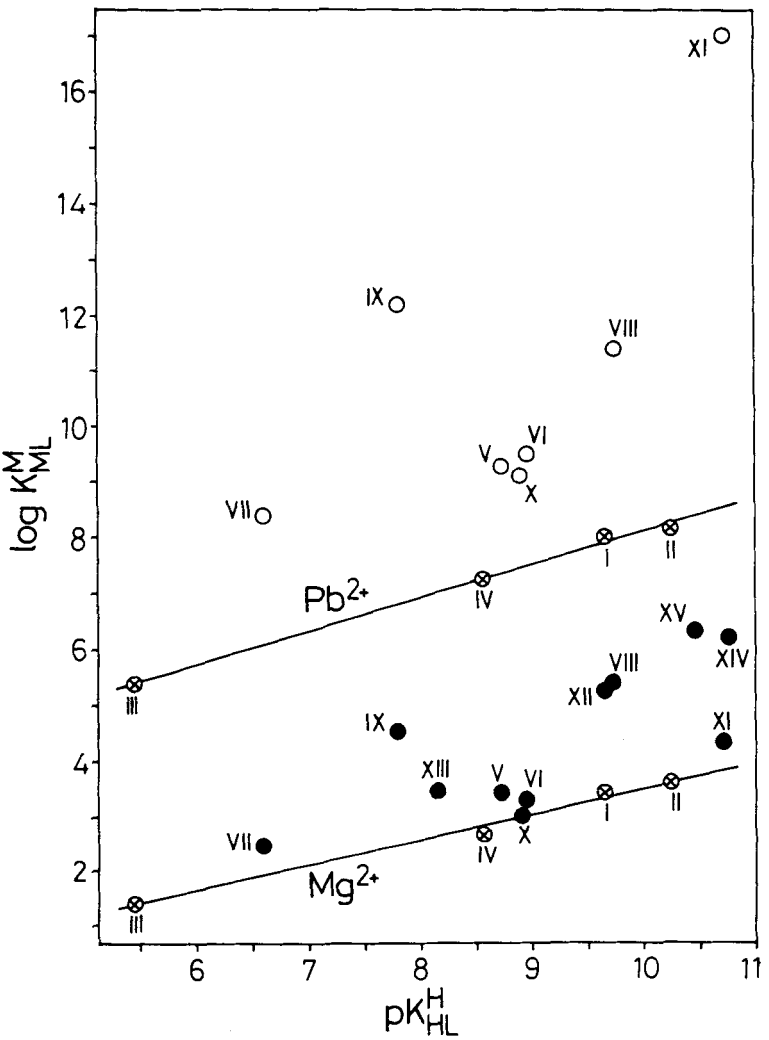

FIGURE 4 Relationship between log K^{M}_{ML} and pK^{H}_{HL} for the Mg^{2+} (●) and Pb^{2+} (○) 1:1 complexes of the N-substituted iminodiacetate ligands of Fig. 3. The least-squares lines are drawn through the data for the iminodiacetates I to IV with a noncoordinating side chain (⊗); the equations for the corresponding least-squares lines are: Mg^{2+}, $y = (0.463 \pm 0.036)x - (1.143 \pm 0.314)$ ($\pm 1\sigma$); Pb^{2+}, $y = (0.594 \pm 0.029)x + (2.174 \pm 0.250)$. The points due to the complexes formed with the potentially tetradentate iminodiacetate derivatives V through XV (●, ○) are inserted for comparison. The plotted equilibrium constant values are from Table I.

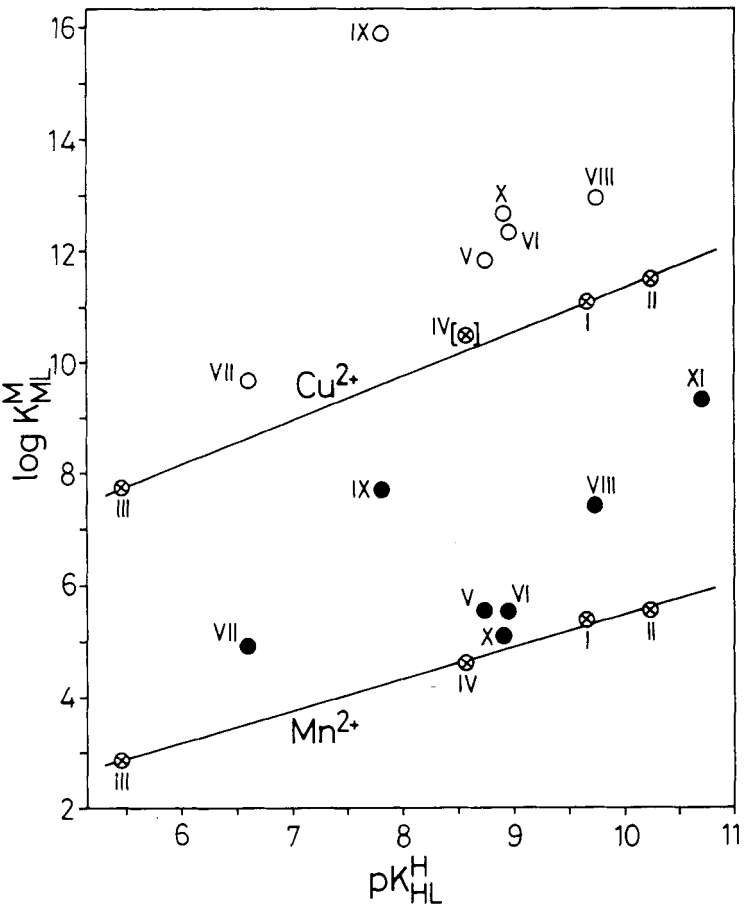

FIGURE 5 Relationship between log K^{M}_{ML} and pK^{H}_{HL} for the Mn^{2+} (●) and Cu^{2+} (○) 1:1 complexes of the N-substituted iminodiacetate ligands of Fig. 3. The least-squares lines are drawn through the data for the iminodiacetates I to IV with a noncoordinating side chain (⊗); regarding Cu^{2+} and the point with ligand IV see text in Section 5.1. The equations for the least-squares lines are: Mn^{2+}, $y = (0.575 \pm 0.029)x - (0.268 \pm 0.250)$ ($\pm 1\sigma$); Cu^{2+}, $y = (0.790 \pm 0.013)x - (3.426 \pm 0.111)$. The points due to the complexes formed with the potentially tetradentate iminodiacetate derivatives V through XI (●, ○) are inserted for comparison. The plotted equilibrium constant values are from Table I.

TABLE II

Logarithms of the deviations of the experimental data (log K^{M}_{ML}) for ligands I to IV (Fig. 3) from the least-squares lines of log K^{M}_{ML} versus pK^{H}_{HL} for the metal-ion complexes considered, together with the slopes of the corresponding least-squares lines (bottom line of the table)[a]

Ligand No.	Side-Chain, *R*	Mg^{2+}	Ca^{2+}	Sr^{2+}	Ba^{2+}	Mn^{2+}	Fe^{2+}	Co^{2+}	Ni^{2+}	Cu^{2+}	Zn^{2+}	Cd^{2+}	Pb^{2+}	Hg^{2+}
I	$-CH_3$	0.11	0.21	0.23	0.21	0.12	0.13[b]	0.15	0.19	0.04	0.08	0.07	0.12	0.05
II	$-(CH_2)_2-C(CH_3)_3$	0.00	−0.10	−0.12	−0.12	−0.07		0.02	−0.19	−0.03	0.02	0.12	−0.09	0.10
III	$-(CH_2)_2-{}^{+}N(CH_3)_3$	0.04	0.02	0.01	0.01	0.01		0.07	−0.04	0.00	0.04	0.09	−0.01	0.07
IV	$-(CH_2)_2-NH-C(O)-O-C_2H_5$	−0.15	−0.12	−0.12	−0.11	−0.06		−0.24	0.04	(0.30)[c]	−0.14	−0.28	−0.01	−0.22
	Slope[d]:	0.46	0.40	0.34	0.25	0.57	0.55[e]	0.48	0.60	0.79	0.54	0.52	0.59	0.65

[a]Calculated from the equilibrium constants in Table I (20°C; I = 0.1 M); see text in Section 5.1.

[b]The straight line is drawn here through the point which is 0.13 log unit below that for ligand I. The above deviation of 0.13 log unit corresponds to the average deviation for ligand I and its complexes with Mn^{2+}, Co^{2+}, Ni^{2+} and Zn^{2+} (see also footnote "e").

[c]This value is not included in the Cu^{2+} baseline for which slope deviation is ±0.01 (see text in Section 5.1).

[d]The standard deviations in the slopes vary from ±0.03 to ±0.06, except for Cu^{2+} (cf. "c"). See also the examples given in Figs. 4 and 5.

[e]Average of the slopes for the Mn^{2+}, Co^{2+}, Ni^{2+}, and Zn^{2+} baselines (see also text in Section 5.1).

positive deviation. We interpret this high stability constant as due to some unsuspected Cu^{2+} substitution for the hydrogen on the carbamate nitrogen to form a five-membered chelate ring. This reaction resembles that occurring with amide nitrogens.[29] Therefore, we have not included the point for ligand IV in the Cu^{2+} baseline, whose slope from the first three ligands is 0.79 ± 0.01. Exclusion of ligand IV would not materially alter the calculated baselines for the other metal ions.

For Fe^{2+} the stability constant for only the first ligand was determined,[1] and in order to include Fe^{2+} in the comparisons, its baseline slope was taken as the average of the slopes for Mn^{2+}, Co^{2+}, Ni^{2+} and Zn^{2+}, and placed so as to pass 0.13 log unit below the point for ligand I. This 0.13 log unit corresponds to the average deviation for the same four metal ions and ligand I from the corresponding baselines.

For all thirteen metal ions of Table II, the baselines for non-coordinating side-chains are so well established that the magnitudes of positive deviations of potentially coordinating side-chains (cf. Figs. 4 and 5) may be used to interpret the extent of side-chain interaction with the given metal ion.

Results for two more iminodiacetate ligands reported by Schwarzenbach *et al.*[1] are excluded from this analysis. They used the stability constant for the ligand with a phenyl side-chain to serve as one point in drawing a baseline. However, since the results for this aniline derivative are not likely to correlate with those for an aliphatic imino nitrogen, they are omitted here. Results for the iminodiacetate ligand with a $-CH_2-C\equiv N$ side-chain do not fit any pattern. We suggest that, depending upon the metal ion, there are varying degrees of metal-ion promoted hydrolysis rendering invalid the reported stability constant values. Indeed, the metal-ion promoted hydrolysis of the $-CH_2-C\equiv N$ side-chain in a macrocyclic complex has been described,[30] and too large stability values for the Cu^{2+} complex of another ligand containing such a group have also been observed.[31]

Furthermore, M(HL) complexes with protonated ligands are also absent from the present analysis because they usually do not chelate as tridentate iminodiacetates. The location of the proton in such M(HL) complexes needs to be specified in each case.

Regarding the results presented for Hg^{2+}, the situation is com-

plicated due to the presence of background 0.1 M KCl,[1] which leads to chloro complexes. However, comparisons of ligand stabilities for Hg^{2+} within this one study should be unaffected by the need to displace Cl^- instead of H_2O from the coordination sphere of Hg^{2+}. Clearly, comparisons with Hg^{2+} stability constants from other studies should only be made with adjustment for the effect of Cl^-.

5.2. Determination of the Stability Enhancement Factors

As described in Section 2, the enhancement factor $(1 + E)$ (see Eq. (8)) may be calculated for any system provided a baseline stability constant, $K^{M}_{ML_o}$, may be estimated. Our procedure for estimating a baseline stability constant on log K^{M}_{ML} versus pK^{H}_{HL} plots is described in Section 5.1. For the present case it employs the pK^{H}_{HL} of the iminodiacetate ligand to find the corresponding log $K^{M}_{ML_o}$ from the least-squares line through points for the first four ligands of Fig. 3 (see also Table II). Four representative examples of log K^{M}_{ML} versus pK^{H}_{HL} plots are shown in Figs. 4 and 5. The logarithmic difference between the observed stability constant (log K^{M}_{ML}) and the baseline stability constant (log $K^{M}_{ML_o}$) for the same ligand pK^{H}_{HL} value results in $\log(K^{M}_{ML}/K^{M}_{ML_o}) = \log\Delta = \log(1 + E)$ as defined in Eq. (9) of Section 2. This quantity appears in Table III for the complexes of the iminodiacetate ligands V to XV.

From Table III it is evident that for the complexes of ligands V to XV all deviations from the least-squares line through the points for the ligands I to IV (Fig. 3; Table II) are positive (see also Figs. 4 and 5), indicating that the side-chain in ligands V to XV has also chelated, at least to some extent, to the metal ion. Due to the experimental error of the constants (Table I), only values for $\log(1 + E) \geq 0.15$ should be interpreted.

A detailed evaluation of the extent of side-chain chelation for ligands V through XV (Fig. 3) is possible from the $\log(1 + E)$ values in Table III in conjunction with Fig. 2 or from Eq. (11) in Section 3. For most cases more than 90% of the complexes in solution have undergone side-chain chelation; i.e., for most cases $\log(1 + E) \geq 1.0$. In fact, for ligands IX and XI with the nine metal ions beyond Mn^{2+}, virtually all complexes contain chelated side-chains; i.e., $\log(1 + E) \geq 3.4$, indicating a formation degree of more than 99.9% (see also Section 5.4).

TABLE III

Logarithms of the enhancement factor $(1 + E)$ (Eqs. (7) and (8)) as determined by the difference between the observed stability constant ($\log K^{M}_{ML}$) and the baseline stability constant ($\log K^{M}_{ML_0}$), i.e. $\log(1 + E) = \log\Delta = \log K^{M}_{ML} - \log K^{M}_{ML_0}$ (Eq. (9)), for several metal-ion complexes of the N-substituted iminodiacetate ligands, $R\text{–}N(CH_2COO^-)_2$, V through XV (Fig. 3)[a]

Ligand No.	Side-Chain, R	log(1 + E)												
		Mg^{2+}	Ca^{2+}	Sr^{2+}	Ba^{2+}	Mn^{2+}	Fe^{2+}	Co^{2+}	Ni^{2+}	Cu^{2+}	Zn^{2+}	Cd^{2+}	Pb^{2+}	Hg^{2+}
V	$-CH_2CH_2-OH$	0.54	1.45	1.46	1.27	0.80	0.8	0.87	1.29	1.53	1.25	1.30	2.05	0.65
VI	$-CH_2CH_2-O-CH_3$	0.30	1.26	1.45	1.35	0.65	0.7	0.82	1.26	1.83	1.22	1.19	2.00	0.96
VII	$-CH_2-C(O)-NH_2$	0.55	1.64	1.44	1.26	1.40	1.0	1.30	1.30	1.04	1.37	1.96	2.31	0.38
VIII	$-CH_2-COO^-$	2.04	2.83	2.33	2.42	2.11	2.3	2.87	2.94	1.84	3.05	3.09	3.44	
IX	$-CH_2CH_2-NH_2$	2.06	1.83	1.55	1.27	3.49	4.3	5.20	6.29	6.31	5.35	4.84	5.41	5.53
X	$-CH_2CH_2-S-CH_3$	0.03	0.09	0.34	0.43	0.25	1.0	1.40	1.90	2.16	1.10	1.57	1.66	3.07
XI	$-CH_2CH_2-S^-$	0.51	0.92	0.64	0.91	3.44	4.6	–[b]	4.58	–[c]	7.70	9.48	8.50	10.06
XII	$-CH_2CH_2COO^-$	1.95	1.49	1.24	1.02									
XIII	$-CH_2CH_2-SO_3^-$	0.84	1.20	1.14	1.00									
XIV	$-CH_2-PO_3^{2-}$	2.44	3.19	2.59	2.69									
XV	$-CH_2CH_2-PO_3^{2-}$	2.63	1.57	1.20	1.06									

[a]The data are calculated from the equilibrium constants given in Table I and the least-squares lines defined in Table II (20°C; I = 0.1 M); see also text in Section 5.2 and the examples plotted in Figs. 4 and 5. Regarding the values for the Fe^{2+} complexes, see footnotes "b" and "e" in Table II.

[b]See footnote "c" in Table I.

[c]See footnote "d" in Table I.

Furthermore, the log $K^{M}_{ML_o}$ versus pK^{H}_{HL} slopes found for Co^{2+}, Ni^{2+}, Cu^{2+}, Zn^{2+}, and Cd^{2+} binding to tridentate iminodiacetates (m = 0.48 to 0.79) in all cases exceed the corresponding slopes for binding to bidentate α-amino acids (m = 0.21 to 0.55).[32] This may be a reflection of the additional carboxylate binding with the iminodiacetates.

5.3. Some Comparisons on the Extent of Side-Chain Interactions

The positive deviations from the least-squares lines (Figs. 4 and 5), i.e., the positive log(1 + E) values for ligands V to XV in Table III, offer many comparisons for assessing relative binding strengths for a variety of ligand donor groups and metal ions. Readers will undoubtedly find their own instructive comparisons; some which strike us most are mentioned here.

Since the iminodiacetate backbone is tridentate, binding of the side-chain requires either a suitable metal-ion geometry to accomodate a quadridentate ligand or a release of one of the backbone carboxylate groups. These steric limitations affect some comparisons. For example, with ligand VIII, nitrilotriacetate, the normal Irving–Williams stability sequence[33] $Ni^{2+} < Cu^{2+} > Zn^{2+}$ occurs in absolute stabilities (log K^{M}_{ML}; Table I) but not in log(1 + E) (Table III) where $Ni^{2+} > Cu^{2+} < Zn^{2+}$. This inversion of the normal order results from the inability of tetragonal Cu^{2+} to bind ligating atoms strongly in an apical position[29] though weak interactions are possible.[34]

For all but three of the eleven ligands V through XV in Table III the sequence is $Ca^{2+} > Mg^{2+}$ in log(1 + E). One exception is ligand IX, with an aminoethyl side-chain showing preference of Mg^{2+} for N donors compared to Ca^{2+}.[35] Comparing the two side-chain pairs, acetate (VIII) to propionate (XII) and methyl phosphate (XIV) to ethyl phosphate (XV), provides an instructive parallel. Ligands VIII and XIV form five-membered chelate rings while ligands XII and XV form six-membered chelates. For the alkaline-earth metal ions ligands VIII and XIV give a maximum in log(1 + E) at Ca^{2+} while the corresponding values for ligands XII and XV monotonically decrease from Mg^{2+} through Ba^{2+}; similar trends have been observed in a different connection.[36]

Comparison of the relative avidity of metal ions for sulfhydryl and oxygen donors by taking the differences of $\log(1 + E)$ values in Table III between the ligand with the thioethyl side-chain (XI) and a ligand with an oxygen donor, either the acetate (VIII) or hydroxyethyl (V) side-chains, gives the results tabulated in Table IV. For both differences three distinct sets of metal ions emerge. The alkaline-earth metal ions yield negative differences in both examples in Table IV; Mn^{2+}, Ni^{2+}, and Fe^{2+} yield small positive differences; and Zn^{2+}, Pb^{2+}, Cd^{2+}, and Hg^{2+} yield large positive differences. The divisions are sharp: the range of values within the first two sets is less than half the span between these sets.

In the hard and soft classification system sulfhydryl donors are classed as soft and oxygen donors as hard.[37] Table IV provides a quantitative measure of the avidity of metal ions for a soft in contrast to a hard ligand donor atom. The results of Table IV yield only a fair correlation with the hard–soft classification of metal ions. All the alkaline-earth metal ions are classed as hard, but so is Mn^{2+}. Ni^{2+}, Fe^{2+}, Zn^{2+}, and Pb^{2+} are classed as borderline while Cd^{2+} and Hg^{2+} are classed as soft. Thus the distinct second set of metal ions in Table IV contains both hard and borderline metal ions while the distinct third set contains both borderline and soft metal ions. This comparison furnishes yet another example of limitations in the hard and soft classification scheme in accounting for properties of metal-ion complexes.[38]

That the sulfhydryl group in ligand XI interacts especially strongly with Cd^{2+} is indicated by the following series of comparisons. For

TABLE IV

Relative affinities of RS^- and $RCOO^-$ or R–OH groups towards several metal ions: sulfhydryl minus oxygen donor atom differences in $\log(1 + E)$ as calculated from the values listed in Table III

$\log(1 + E)_{XI} - \log(1 + E)_{VIII}$	Set of Metal Ions	$\log(1 + E)_{XI} - \log(1 + E)_{V}$
−1.7 to −1.5	Mg^{2+}, Ca^{2+}, Sr^{2+}, Ba^{2+}	−0.8 to 0.0
1.3 to 2.4	Mn^{2+}, Ni^{2+}, Fe^{2+}	2.6 to 3.9
4.7 to 6.4	Zn^{2+}, Pb^{2+}, Cd^{2+}, (Hg^{2+})	6.4 to 8.1 (9.4)

ligands V through XI in Table III the log(1 + E) values are for $Ni^{2+} \geq Zn^{2+}$ except for ligand XI, where Zn^{2+} is more strongly bound by 3.2 log units. The log(1 + E) values for the Cd^{2+} and Zn^{2+} complexes are the same within 0.6 log units except with ligand XI, which binds Cd^{2+} 1.8 log units more strongly. All the Pb^{2+} complexes exhibit greater log(1 + E) values than Cd^{2+}, except for ligand XI which is 1.0 log units stronger for Cd^{2+}. The difference in log(1 + E) values for sulfhydryl (XI) and thioether (X) groups falls within the narrow range of 6.7 to 7.0 log units for Zn^{2+}, Pb^{2+}, and Hg^{2+}, but is 7.9 log units for Cd^{2+}.

The indicated high affinity of Cd^{2+} for sulfhydryl groups dictates caution when using Cd^{2+} as a general probe for Ca^{2+} (a nonsulfur binder) in proteins.[35] The especially strong binding of Cd^{2+} to the sulfhydryl side-chain (XI), where it is second only to Hg^{2+} in log(1 + E) in Table III, does not extend to the thioether side-chain (X), where Cd^{2+} gives only the fifth highest value. Thus soft Cd^{2+} binding to the soft sulfhydryl group side-chain is second only to soft Hg^{2+}, but Cd^{2+} binding to the also soft thioether group side-chain of the same ring size trails behind borderline Pb^{2+}, Ni^{2+}, and Cu^{2+}. Once again, oversimplifications in the hard–soft classification scheme become apparent. Binding of metal ions to the thioether group in the amino acids methionine and S-methylcysteine have received review.[28]

5.4. The Special Binding Properties of Ligand XI: N-(2-Mercaptoethyl)iminodiacetate or N,N-Bis(carboxymethyl)-2-aminoethanethiolate?

Until now the ligands I through XV of Fig. 3 have been considered as substituted iminodiacetates. As discussed in the preceding section, however, ligand XI carries the strongly chelating sulfhydryl side-chain. Hence, for this ligand it may be more appropriate to consider the fundamental backbone to be 2-aminoethanethiolate with the two carboxylate side-chains as the more weakly chelating groups. We now test quantitatively this alternative viewpoint for ligand XI, and we conclude that it depends upon the metal ion which ligand grouping provides the more strongly binding backbone.

For ligand XI, N-(2-mercaptoethyl)iminodiacetate, the pK_a values for the sulfhydryl and ammonium groups[1] of 8.17 and 10.79

are virtually identical to those of 8.21 and 10.71 for 2-aminoethanethiolate.[39] The near identity of the pair of pK_a values in the two ligands permits a direct comparison of their stability constants. The differences in stability constant logarithms between ligand XI and 2-aminoethanethiolate follow each metal ion in parentheses: Mg^{2+} (2.0), Ca^{2+} (2.7), Sr^{2+} (2.1), Ba^{2+} (2.2), Ni^{2+} (3.7), Zn^{2+} (6.0), Cd^{2+} (5.8), and Pb^{2+} (5.9). These differences represent the enhancement factors $\log(1 + E)$ for metal-ion binding due to the two carboxylate groups on ligand XI over the binding to the 2-aminoethanethiolate backbone. These values may be compared to those for ligand XI in Table III, which represent enhancement factors due to the sulfhydryl side-chain over binding to the iminodiacetate backbone. The differences between the enhancement factors in Table III minus those listed above in this paragraph are as follows: Mg^{2+} (−1.5), Ca^{2+} (−1.8), Sr^{2+} (−1.5), Ba^{2+} (−1.3), Ni^{2+} (0.9), Zn^{2+} (1.8), Cd^{2+} (3.7), and Pb^{2+} (2.6).

The negative values for the four alkaline-earth metal ions reveal that these ions may be viewed as coordinating to ligand XI as a substituted iminodiacetate with a weakly coordinating sulfhydryl group. The positive values for the other metal ions indicate that they coordinate primarily to the 2-aminoethanethiol portion of ligand XI with a weaker interaction with the two carboxylate groups. The ambivalent properties of ligand XI are thus nicely seen.

6. INTRAMOLECULAR EQUILIBRIA IN COMPLEXES WITH α-SUBSTITUTED ACETATE LIGANDS

The binding sites in the side-chains of the N-substituted iminodiacetate ligands of Fig. 3 significantly enhance complex stability in most cases (cf. Table III); i.e., equilibrium (1) in 86 of a total of 104 cases has a formation degree of more than 90% of ML_{cl} and is thus largely on its right side. Due to this large displacement of equilibrium (1), in the discussions of Sections 5.3 and 5.4 the stability enhancement factor $1 + E$ ($= 10^{\log\Delta}$; see Eqs. (8) and (9)) was used to characterize the properties of the ligands.

In cases where more equivalent portions of the isomers in equilibrium (1) are present it may be more helpful to consider the fraction, f, of the closed isomer (Eq. (11)) or its 100-fold value,

i.e., the formation degree of the chelated isomer, % ML_{cl}. As an example of such a situation we consider now the complexes of the α-substituted acetate ligands shown in Fig. 6. All five ligands of Fig. 6 contain an O or S binding site in the α-position; hence, they are potentially able to form five-membered chelates, but whether they do so will depend on the kind of metal ion employed.

For the first three ligands of Fig. 6 the data[40] are plotted in Fig. 7 for their Mn^{2+}, Cu^{2+} and Zn^{2+} complexes, together with the corresponding log K^{M}_{ML} versus pK^{H}_{HL} plots for several simple monocoordinating carboxylate ligands which furnish the baselines. The vertical differences to these baselines from the points due to $M(HOAc)^+$, $M(EtSAc)^+$ and $M(Thfc)^+$ correspond to the logarithm of the enhancement factors, i.e., to $\log(1 + E)$ as already described in Section 2. The detailed evaluation of these data is collected in Table V, together with the corresponding information for the $M(Thtc)^+$ and $M(Dtc)^+$ complexes taken from earlier work.[11]

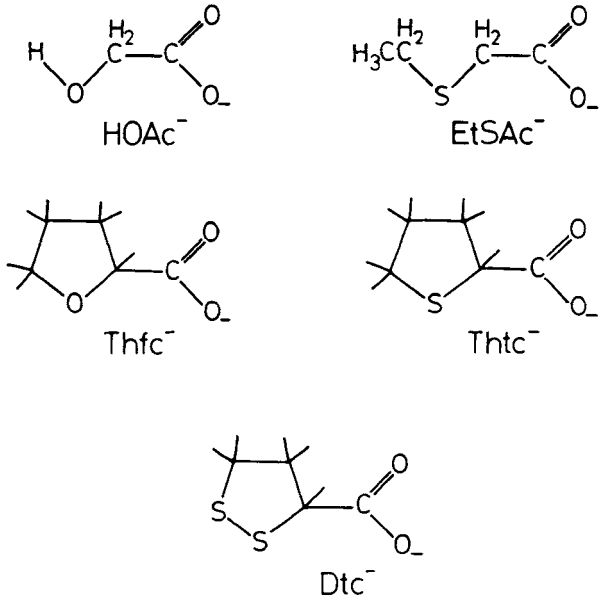

FIGURE 6 Structures of the α-substituted acetate ligands considered in Section 6: α-hydroxyacetate ($HOAc^-$), α(S-ethylthio)acetate (or S-carboxymethyl ethylmercaptan; $EtSAc^-$), tetrahydrofuran-2-carboxylate ($Thfc^-$), tetrahydrothiophene-2-carboxylate ($Thtc^-$), and 1,2-dithiolan-3-carboxylate (or tetranorlipoate; Dtc^-).

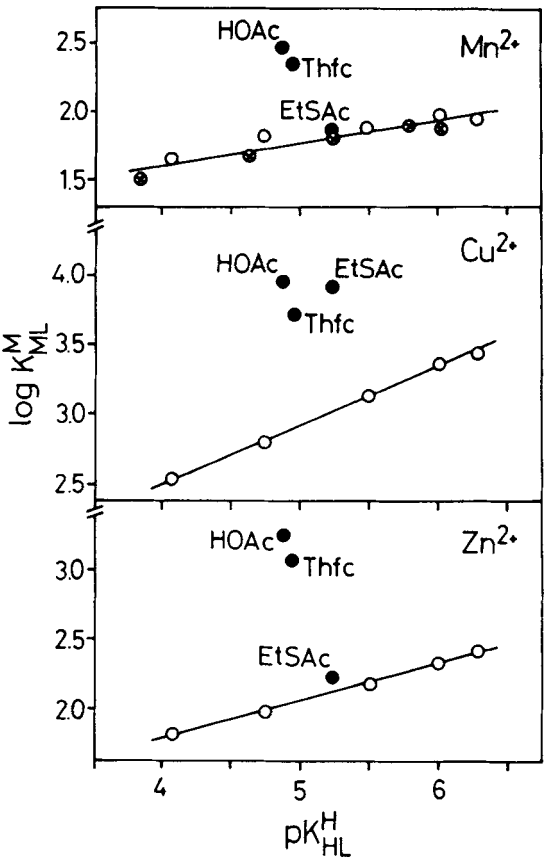

FIGURE 7 Relationship between log K^{M}_{ML} and pK^{H}_{HL} for the 1:1 complexes of Mn^{2+} (top), Cu^{2+} (middle) and Zn^{2+} (bottom) with the monodentate (○) carboxylate ligands (from left to right) chloroacetate, formate, β-chloropropionate, acetate and propionate; in case of Mn^{2+} are in addition the points of five monodentate benzoate ligands (⊗) inserted. The equations for the corresponding least-squares lines are: Mn^{2+}, $y = (0.159 \pm 0.023)x + (0.971 \pm 0.119)$ ($\pm 1\sigma$); Cu^{2+}, $y = (0.424 \pm 0.007)x + (0.797 \pm 0.040)$; and Zn^{2+}, $y = (0.264 \pm 0.011)x + (0.736 \pm 0.059)$. For comparison are also inserted the corresponding data for the complexes of some potentially bidentate α-substituted acetate ligands of Fig. 6 (●); see text in Section 6. All plotted equilibrium constant values are from Table I of Ref. 40; they refer to 50% (v/v) aqueous dioxane solutions at 25°C and $I = 0.1$ M, $NaClO_4$.

TABLE V

Extent of chelate formation in M^{2+} 1:1 complexes of α-substituted acetate ligands (Fig. 6) in 50% (v/v) aqueous dioxane at 25°C and I = 0.1 M ($NaClO_4$ or $NaNO_3$)[a]

L^-	M^{2+}	log K^M_{ML}	log K^M_{MLo}	log(1 + E) = logΔ (Eq. (9))	K_I = E (Eqs. (1) and (7))	%ML_{cl} (f · 100/cf. Eq. (11))
$HOAc^-$	Mn^{2+}	2.48 ± 0.06	1.75 ± 0.02	0.73 ± 0.06	4.4 ± 0.8	81 ± 3
	Cu^{2+}	3.96 ± 0.04	2.87 ± 0.02	1.09 ± 0.04	11.3 ± 1.3	92 ± 1
	Zn^{2+}	3.26 ± 0.04	2.02 ± 0.02	1.24 ± 0.04	16.4 ± 1.8	94 ± 1
$EtSAc^-$	Mn^{2+}	1.85 ± 0.05	1.80 ± 0.02	0.05 ± 0.05	0.12 ± 0.14	11 ± 11
	Cu^{2+}	3.92 ± 0.03	3.02 ± 0.02	0.90 ± 0.04	6.9 ± 0.7	87 ± 1
	Zn^{2+}	2.22 ± 0.03	2.12 ± 0.02	0.10 ± 0.04	0.26 ± 0.10	21 ± 7
$Thfc^-$	Mn^{2+}	2.36 ± 0.05	1.76 ± 0.02	0.60 ± 0.05	3.0 ± 0.5	75 ± 3
	Cu^{2+}	3.72 ± 0.03	2.90 ± 0.02	0.82 ± 0.04	5.6 ± 0.6	85 ± 1
	Zn^{2+}	3.07 ± 0.03	2.04 ± 0.02	1.03 ± 0.04	9.7 ± 0.9	91 ± 1
$Thtc^-$	Mn^{2+}	1.80 ± 0.05		~0	~0	≤20
	Cu^{2+}	4.31 ± 0.03		1.16 ± 0.04	13.5	93 ± 1
	Zn^{2+}	2.35 ± 0.03		0.15 ± 0.04	0.41	29 ± 6
	Cd^{2+}	2.68 ± 0.02		0.34 ± 0.03	1.2	54 ± 3
	Pb^{2+}	3.32 ± 0.03		0.40 ± 0.04	1.5	60 ± 3
Dtc^-	Mn^{2+}	1.87 ± 0.03		~0.04	~0.1	~9(≤20)
	Cu^{2+}	3.07 ± 0.03		0.23 ± 0.04	0.70	41 ± 5
	Zn^{2+}	2.14 ± 0.03		0.15 ± 0.04	0.41	29 ± 6
	Cd^{2+}	2.10 ± 0.04		~0	~0	≤11
	Pb^{2+}	2.76 ± 0.04		0.31 ± 0.04	1.04	51 ± 5

[a]The stability constants, log K^M_{ML}, for the first three ligands are from Table I in Ref. 40 ($NaClO_4$); the corresponding values for log K^M_{MLo} were calculated from the baseline equations given in Fig. 7 and the ligand pK^H_{HL} values: $pK^H_{H(HOAc)}$ = 4.88 ± 0.03, $pK^H_{H(EtSAc)}$ = 5.24 ± 0.01, and $pK^H_{H(Thfc)}$ = 4.95 ± 0.01 (Ref. 40). The error limits for both log K values are estimates; the errors for all other data were calculated according to the error propagation after Gauss. The results for $Thtc^-$ and Dtc^- are taken from Table 2 of Ref. 11; the error limits given for %ML_{cl} contain also in these cases a possible baseline error of ±0.02 log units.

The intramolecular equilibrium constants K_I (Eq. (1)) and the corresponding percentages for the chelated isomers, % ML_{cl}, in Table V reveal that hydroxy groups, ether, and thioether moieties have approximately the same affinity towards Cu^{2+}. If the data for the sterically most comparable $Cu(Thfc)^+$ and $Cu(Thtc)^+$ complexes are considered, a slightly larger affinity of the thioether group for Cu^{2+} is born out. This result agrees well with the ether and thioether systems considered in Table III (ligands VI and X). Of further interest is a comparison of the data for $Cu(Thtc)^+$ and $Cu(Dtc)^+$: it becomes thus evident that the thioether group coordinates Cu^{2+} much more avidly than a sulfur in a disulfide bridge. The corresponding result is seen for Cd^{2+}, while for Zn^{2+} and Pb^{2+} the affinities of the thioether and disulfide groups correspond to each other.

Mn^{2+} has a pronounced coordination tendency for O-substituted α-acetates, but only a weak one for a corresponding S-binding site (Table V). The affinity of Zn^{2+} for the latter sites is certain though it is also less pronounced than for the O-binding sites. Comparison of $\%ML_{cl}$ for $Zn(Thtc)^+$ and $Cd(Thtc)^+$ shows that Cd^{2+} is more strongly interacting with a thioether sulfur than Zn^{2+}. All these conclusions parallel the observations described in Section 5 for Table III.

Further comparisons for the data in Table V and possible interrelations with those in Table III are left to the reader. The essential point demonstrated by the results of Table V is that there are situations for equilibrium (1) which allow the formation of only traces of one isomer, as well as those leading to approximately comparable portions of the two isomers.

7. CONCLUDING REMARKS

The discussion of the examples presented in Sections 5 (Table III) and 6 (Table V) has shown that, depending on the size of the effects, it may be more useful, in considering the situation for equilibrium (1), to apply for strong chelation the logarithm of the stability enhancement factor, log $(1 + E)$, and for weak chelation the fraction f of the closed form, i.e., $\%ML_{cl}$ (see also Fig. 2). There is of course no limit to applying the two descriptions. Most

importantly, Eqs. (7), (8), (9) and (11) allow a quantitative description of isomeric equilibria which is quite general.

This last point has to be emphasized: In this Comment only intramolecular equilibria for binary complexes have been considered; however, exactly the same type of evaluation is possible for intramolecular ligand–ligand interactions in mixed ligand complexes as that indicated in equilibrium (21):

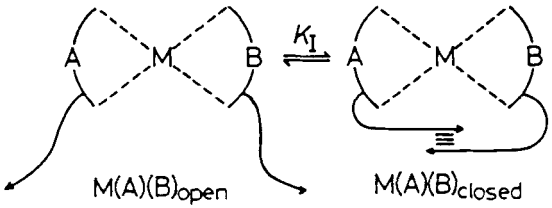

(21)

Examples of such evaluations exist already in the literature.[41] The position of equilibrium (21) has been quantified for intramolecular ionic interactions between oppositely charged groups,[42] as well as for hydrophobic[11–13,16] and stacking interactions.[8,12–14,16,43,44]

From Fig. 2 it is evident that significant formation degrees of a closed species, be it in equilibrium (1) or in (21), are connected only with small changes in free energy (ΔG^0). Considering reactive intermediates in metal-ion catalyzed or facilitated reactions,[45] this important point should be kept in mind when discussing technological processes as well as biological systems.

Acknowledgment

The support of this research by the Swiss National Science Foundation is gratefully acknowledged.

R. BRUCE MARTIN
Chemistry Department,
University of Virginia,
Charlottesville, Virginia 22903

HELMUT SIGEL
Institute of Inorganic Chemistry,
University of Basel,
Spitalstrasse 51,
CH-4056 Basel, Switzerland

References

1. G. Schwarzenbach, G. Anderegg, W. Schneider and H. Senn, Helv. Chim. Acta **38**, 1147 (1955).
2. R. S. Taylor and H. Diebler, Bioinorg. Chem. **6**, 247 (1976).
3. C. Miller Frey and J. E. Stuehr, J. Am. Chem. Soc. **100**, 139 (1978).
4. Y. H. Mariam and R. B. Martin, Inorg. Chim. Acta **35**, 23 (1979).
5. K. H. Scheller, F. Hofstetter, P. R. Mitchell, B. Prijs and H. Sigel, J. Am. Chem. Soc. **103**, 247 (1981).
6. H. Sigel, R. Tribolet, R. Malini-Balakrishnan and R. B. Martin, Inorg. Chem. **26**, 2149 (1987).
7. H. Sigel, Eur. J. Biochem. **165**, 65 (1987).
8. H. Sigel, Chimia **41**, 11 (1987).
9. H. Sigel, K. H. Scheller, V. M. Rheinberger and B. E. Fischer, J. Chem. Soc., Dalton Trans. 1022 (1980).
10. H. Sigel, Experientia **37**, 789 (1981).
11. H. Sigel, Angew. Chem. **94**, 421 (1982); Angew. Chem. Int. Ed. Engl. **21**, 389 (1982).
12. B. E. Fischer and H. Sigel, J. Am. Chem. Soc. **102**, 2998 (1980).
13. H. Sigel, B. E. Fischer and E. Farkas, Inorg. Chem. **22**, 925 (1983).
14. R. Tribolet, R. Malini-Balakrishnan and H. Sigel, J. Chem. Soc., Dalton Trans. 2291 (1985).
15. P. L. Yeagle, W. C. Hutton and R. B. Martin, J. Am. Chem. Soc. **97**, 7175 (1975).
16. S.-H. Kim and R. B. Martin, J. Am. Chem. Soc. **106**, 1707 (1984).
17. A. E. Martell and M. Calvin, *Chemistry of the Metal Chelate Compounds* (Prentice-Hall, Englewood Cliffs, New Jersey, 1952).
18. H. Erlenmeyer, R. Griesser, B. Prijs and H. Sigel, Helv. Chim. Acta **51**, 339 (1968).
19. J. Bjerrum, Chem. Reviews **46**, 381 (1950).
20. M. Calvin and K. W. Wilson, J. Am. Chem. Soc. **67**, 2003 (1945).
21. (a) H. Irving and H. Rossotti, Acta Chem. Scand. **10**, 72 (1956). (b) F. J. C. Rossotti, "The Thermodynamics of Metal Ion Complex Formation in Solution," in *Modern Coordination Chemistry*, eds. J. Lewis and R. G. Wilkins (Interscience Publishers Inc., New York, 1960), p. 51.
22. J. G. Jones, J. B. Poole, J. C. Tomkinson and R. J. P. Williams, J. Chem. Soc. 2001 (1958).
23. H. Sigel and Th. Kaden, Helv. Chim. Acta **49**, 1617 (1966).
24. P. Y. Sollenberger and R. B. Martin, in *The Chemistry of the Amino Group*, ed. Saul Patai (John Wiley, New York, 1968), p. 349–406.
25. E. Nieboer and W. A. E. McBryde, Can. J. Chem. **48**, 2549 (1970).
26. E. Nieboer and W. A. E. McBryde, Can. J. Chem. **48**, 2565 (1970).
27. G. Schwarzenbach, H. Ackermann and P. Ruckstuhl, Helv. Chim. Acta **32**, 1175 (1949).
28. R. B. Martin, Met. Ions Biol. Syst. **9**, 1 (1979).
29. H. Sigel and R. B. Martin, Chem. Reviews **82**, 385 (1982).
30. (a) T. A. Kaden, Topics Curr. Chemistry **121**, 157 (1984). (b) W. Schibler and T. A. Kaden, J. Chem. Soc., Chem. Commun. 603 (1981).
31. H. Gampp, D. Haspra, M. Maeder and A. D. Zuberbühler, Inorg. Chem. **23**, 3724 (1984).
32. R. B. Martin, Met. Ions Biol. Syst. **23**, 123 (1988).

33. (a) H. Irving and R. J. P. Williams, Nature (London) **162**, 746 (1948). (b) H. Irving and R. J. P. Williams, J. Chem. Soc. 3192 (1953).
34. (a) E. W. Wilson, Jr., M. H. Kasperian and R. B. Martin, J. Am. Chem. Soc. **92**, 5365 (1970). (b) H. Gampp, H. Sigel and A. D. Zuberbühler, Inorg. Chem. **21**, 1190 (1982).
35. R. B. Martin, Met. Ions Biol. Syst. **17**, 1 (1984).
36. H. Sigel, K. H. Scheller and B. Prijs, Inorg. Chim. Acta **66**, 147 (1982).
37. R. G. Pearson (Ed.), *Hard and Soft Acids and Bases* (Dowden, Hutchinson and Ross, Stroudsberg, Pennsylvania, 1973).
38. R. B. Martin, Met. Ions Biol. Syst. **20**, 21 (1986).
39. R. M. Smith and A. E. Martell, *Critical Stability Constants*, Volume 2 (Plenum Press, New York, 1975).
40. H. Sigel, R. Griesser, B. Prijs, D. B. McCormick and M. G. Joiner, Arch. Biochem. Biophys. **130**, 514 (1969).
41. H. Sigel, "Stability, Structure and Reactivity of Mixed Ligand Complexes in Solution," in *Coordination Chemistry—20*, ed. D. Banerjea (IUPAC; Pergamon Press, Oxford and New York, 1980), p. 27–45.
42. R. Tribolet, H. Sigel and K. Trefzer, Inorg. Chim. Acta **79**, 278 (1983).
43. O. Yamauchi and A. Odani, J. Am. Chem. Soc. **107**, 5938 (1985).
44. H. Sigel, R. Malini-Balakrishnan and U. K. Häring, J. Am. Chem. Soc. **107**, 5137 (1985).
45. V. Scheller-Krattiger and H. Sigel, Inorg. Chem. **25**, 2628 (1986).